Inorganic Chemistry

Article

pubs.acs.org/IC

Investigation of in Situ Oxalate Formation from 2,3-Pyrazinedicarboxylate under Hydrothermal Conditions Using Nuclear Magnetic Resonance Spectroscopy

Karah E. Knope,[†] Hiroshi Kimura,[‡] Yoshiro Yasaka,[‡] Masaru Nakahara,*[,‡] Michael B. Andrews,[†] and Christopher L. Cahill*[,†]

[†]Department of Chemistry, The George Washington University, 725 21st Street NW, Washington, D.C. 20052, United States

[‡]Institute for Chemical Research, Kyoto University, Gokasho, Uji, Kyoto 611-011, Japan

Supporting Information

ABSTRACT: We have investigated the assembly of a two-dimensional coordination polymer, $Nd_2(C_6H_2N_2O_4)_2(C_2O_4)(H_2O)_2$, that has been prepared from the hydrothermal reaction of $Nd(NO_3)_3{\cdot}6H_2O$ and 2,3-pyrazinedicarboxylic acid (H_2pzdc). In situ oxalate formation as observed in this system has been been investigated using ^{1}H and ^{13}C nuclear magnetic resonance spectroscopy, and a pathway for $C_2O_4^{2-}$ anion formation under hydrothermal conditions has been elucidated. The oxalate ligands found in $Nd_2(C_6H_2N_2O_4)_2(C_2O_4)(H_2O)_2$ result from the oxidation of H_2pzdc, which proceeds through intermediates, such as 2-pyrazinecarboxylic acid (2-pzca), 2-hydroxyacetamide, 3-amino-2-hydroxy-3-oxopropanoic acid, 2-hydroxymalonic acid, 2-oxoacetic acid (glyoxylic acid), and glycolic acid. The species are generated through a ring-opening that occurs via cleavage of the C−N bond of the pyrazine ring, followed by hydrolysis/oxidation of the resulting species.

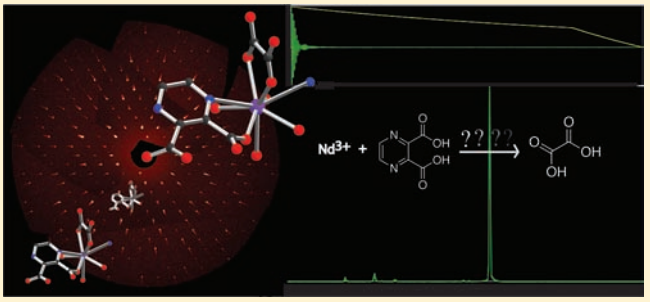

INTRODUCTION

The synthesis and design of inorganic/organic coordination polymers with desired structure types and functions has become an extensive area of research. Yaghi et al reported in 2005 that there were some 12 000 polymeric metal−organic structures in the Cambridge Structural Database (CSD)[1,2] Since then, the number of hybrid inorganic/organic compounds in the CSD (Ver. 5.32, Nov. 2010) has grown to approximately 38 000 (inclusive of the d- and f-block elements). Interest in these materials stems not only from their propensity to form extended structures with a range of structural motifs and topologies but also their potential application to areas such as gas storage, drug delivery, ion exchange, separations, sensing, and catalysis.[3−15] Metal−organic structures have traditionally been prepared through the direct coordination of either presynthesized or commercially available ligands to metal ions.[16,17] More recently, however, synthesis efforts during the search for such novel inorganic−organic materials have inadvertently discovered an inventory of in situ metal/ligand reactions[18,19] that include, among others, carbon−carbon bond formation,[20,21] hydroxylation,[22] cycloaddition,[23] triazole and tetrazole formation,[24−26] transformation of inorganic and organic sulfur,[27−30] hydrolysis,[31−34] oxidation−hydrolysis,[35,36] decarboxylation,[37−41] and acylation.[42,43] Such "in situ ligand syntheses" often result in phases that are not obtainable by starting with preformed ligands. Although some of these reactions can be rationalized after the fact, a priori prediction and ultimately capitalizing on this phenomena remains challenging, in large part due to the serendipity of observations and the lack of dedicated mechanistic studies.

In situ formation of organic linkers typically relies on the rearrangement or cleavage of organic compounds, a process that is commonly metal-mediated. The rearranged organic species are then observed in crystalline reaction products. This notion of generating ligands in situ was first proposed by Blake et al. in 1997.[44] Since their unexpected observation of the in situ cyclization of 1,2-trans-(4-pyridyl)ethane to 1,2,3,4-tetrakis(4-pyridyl)cyclobutane, in situ ligand synthesis has rapidly become an effective, yet still poorly understood, approach to crystal engineering.[19] Because of the "black box" nature of hydro(solvo)thermal syntheses and the inherent difficulties associated with monitoring these systems, most accounts of in situ ligand formation have focused primarily on the topologies and physiochemical properties of the resulting coordination compounds. Synthetic variables that may promote in situ metal−ligand transformations have rarely been explored systematically, and even fewer examples exist wherein proposed intermediates have been characterized. Furthermore, the absence of in depth inquiries addressing both solution-phase and solid-state speciation has significantly limited the ability of

Received: January 13, 2012
Published: February 24, 2012

materials chemists to elucidate and thereby rationalize mechanisms of in situ ligand reactions under nonambient conditions.

A frequently reported in situ phenomenon in coordination polymer and MOF literature is the formation of oxalate anions ($C_2O_4^{2-}$) under hydro(solvo)thermal conditions, a fairly comprehensive listing of which is provided in the Supporting Information. As seen in Table S1 (Supporting Information), in situ oxalate formation has been observed under a range of synthetic conditions, in the presence of various metal cations and with an assortment of organic ligands. Moreover, several pathways have been proposed for oxalate formation, yet most can be described as either (1) the decarboxylation of carboxylate functionalized organic species, followed by the subsequent reductive coupling of CO_2, or (2) the decomposition or oxidation of an organic species. Additionally, instances of the oxidative coupling of methanol or ethanol to yield oxalate have been reported. Table S1 (Supporting Information) does not include examples wherein CO_2 was fixed directly from the atmosphere (with two exceptions) or through intentional introduction. We also note a number of studies that have observed decarboxylation of similar species, but did not result in oxalate formation.[40,45,46]

Our research group has reported several instances of oxalate formation under hydrothermal conditions. We have, in fact, proposed decarboxylation and subsequent reductive coupling of CO_2,[13,47−49] yet as we will develop herein, these suggestions were indeed a bit speculative considering that these reactions took place under highly oxidizing conditions. Like many other studies, however, our efforts have relied on ex situ crystallographic characterization and, in turn, an "after the fact" mechanistic discussion based on identifying ordered organic species present in solid-state reaction products. One particular example was the oxidation of DABCO (1,4-diazabicylo[2.2.2]-octane) to form both oxalate and glycolate anions after 14 days at 180 °C.[50] Interestingly, we were able to identify decomposition species (piperazine, *N*,*N*′-dinitrosopiperazine, as well as glycolate and oxalate anions) within crystalline products via quenching of the reaction as a function of time. While this afforded for determination of a reaction mechanism, this study was still an ex situ investigation of an in situ phenomenon.

More recently, Soares-Santos et al. have reported the synthesis of $[Ln(H_2pzdc)_2(ox)(H_2O)_2]_n$ [Ln = Ce, Nd, Sm, Eu, Gd, Tb, or Er] from lanthanide nitrates and H_2pzdc under hydrothermal conditions.[51] They proposed that the oxalate ligand observed in the crystalline reaction product resulted from the decomposition of H_2pzdc, as shown in Scheme 1. In

Scheme 1. Formation of 2-Pyrazinecarboxylate (2-pzca) and Oxalate (ox) via Decomposition of H_2pzdc As Reported by Soares-Santos et al.[51] and Cahill et al.[49]

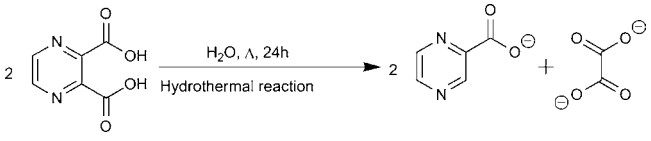

support of this, they also isolated $[Tb_2(2\text{-pzca})4(ox)(H_2O)_6]\cdot 10H_2O$ as a secondary phase, thus "unequivocally proving H_2pzdc decomposed into ox^{2-} and 2-$pzca^-$." Similarly, and prior to their study, we reported the synthesis of $Th(ox)_2(H_2O)_2\cdot 2H_2O$ from hydrothermal reactions of $Th(NO_3)_4$, $Cu(NO_3)_2$, and 2,3-pyrazinedicarboxylic acid (H_2pzdc).[49] We also proposed that decarboxylation of H_2pzdc yielded 2-pyrazinecarboxylic acid and CO_2(g) and suggested that oxalate ligands were believed to result from the subsequent coupling of CO_2 species. Whereas we observed the monocarboxylate (2-pzca) in one of the reaction products, $Cu(2\text{-pzca})(NO_3)(H_2O)$,[49] it was perhaps a bit short-sighted for us to have considered reductive coupling as the only source of oxalate as this reaction was under acidic and oxic conditions.

As highlighted by these reports and likewise prevalent within most accounts of in situ ligand formation, discussions of pathways and mechanisms of oxalate formation have predominately been based on crystallographic observations made in the solid state; relatively few studies have explored solution speciation. As will be presented in this contribution, solution-phase studies, when coupled to solid state characterization, allow for more detailed mechanistic investigation and indeed suggest an entirely different mechanism for oxalate formation.

Materials chemists have been utilizing in situ techniques to elucidate reaction pathways for some time. Indeed, XRD and spectroscopic techiques have been employed in the study of porous and other materials.[52−55] Moreover, physical chemists as well as geochemists have long employed spectroscopic techniques for monitoring the kinetics and reaction pathways of solution-phase organic transformations that occur in super- and subcritical water.[46,56,57] Nakahara et al., for example, have explored a variety of noncatalytic hydrothermal organic reactions, including decarbonylation,[58−60] decarboxylation,[60] and carbon−carbon bond formation,[61] using NMR spectroscopy. Reported herein is an extension of these techniques to inorganic−organic materials synthesis and, in particular, in situ oxalate formation. In an effort to progress our understanding of hydro(solvo)thermal metal−ligand reactions beyond speculative mechanisms or those inferred from crystallographic studies of the solid sate, solution-phase speciation and thus the chemical evolution of H_2pzdc to oxalate have been monitored using ^1H and ^{13}C NMR spectroscopy. Under hydrothermal conditions and in the presence of Nd^{3+}, the oxidation of H_2pzdc proceeds through intermediates, such as 2-pyrazinecarboxylic acid (2-pzca), 2-hydroxyacetamide, 3-amino-2-hydroxy-3-oxopropanoic acid, 2-hydroxymalonic acid, 2-oxoacetic acid (glyoxylic acid), and glycolic acid, and ultimately yields oxalate ligands that are observed in $Nd_2(C_6H_2N_2O_4)_2(C_2O_4)(H_2O)_2$. Whereas the synthesis and structure of this compound have been reported previously by Soares-Santos et al., the present contribution is the first in situ NMR study of oxalate formation to explain the origin of the oxalate ligands observed in this material. Consequently, we provide new mechanistic information that suggests a ring-opening/hydrolysis-oxidation pathway that may very likely explain numerous reports of oxalate formation. Detailed mechanistic information, such as provided herein, will be key to moving in situ ligand synthesis from serendipity to a viable synthesis tool.

EXPERIMENTAL SECTION

Although **1** has been previously prepared and characterized, the synthetic conditions under which we isolated the compound are described for the purposes of discussion, as is a brief overview of the crystal structure.

Synthesis. Compound **1**, $Nd_2(C_6H_2N_2O_4)_2(C_2O_4)(H_2O)_2$: Neodymium nitrate hexahydrate (0.171 g, 0.39 mmol), 2,3-pyrazinedicarboxylic acid (0.069 g, 0.41 mmol), and distilled water (5 g, 278 mmol) were placed into a 23 mL Teflon-lined Parr bomb in the molar ratio of 1.0:1.0:992, respectively (pH 1.7). The reaction vessel was

dx.doi.org/10.1021/ic3000944 | Inorg. Chem. 2012, 51, 3883−3890

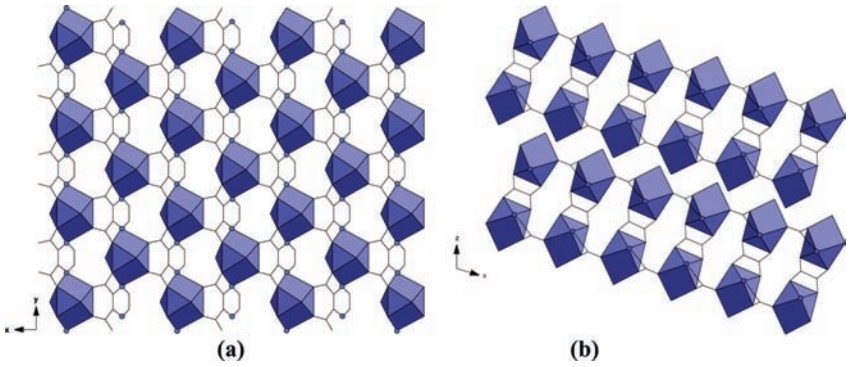

Figure 1. Polyhedral representations of **1** (a) viewed down the [001] direction illustrating the topology of the 2-D sheets and (b) highlighting the linkage of the sheets along [100] via oxalate ligands. Purple polyhedra are discrete nine-coordinate Nd^{3+} centers. Blue spheres and black lines represent nitrogen and carbon atoms of the linker molecules.

then sealed and heated statically at 120 °C for 1 day. Upon cooling to room temperature, a cloudy white liquid (pH 1.9) was decanted and a faint purple crystalline solid was obtained. The product was washed with distilled water, followed by ethanol, and then allowed to air-dry at room temperature. Yield: 13% (based on neodymium). A single crystal was isolated from the bulk product for X-ray structure determination. Powder X-ray diffraction data were collected using a Rigaku Miniflex diffractometer (Cu Kα, 10−60°) to compare observed and calculated patterns to (a) verify that the single crystal was representative of the bulk and (b) identify impurities when necessary. Elemental analysis of **1** (Galbraith Laboratories, Knoxville, TN) is as follows: observed (calculated): C, 22.29% (22.58%); H, 1.08% (1.26%); N, 7.50% (7.52%). Reactions analogous to that described above that were conducted over 3 h, 5 h, and 3 days gave compound **1** in varying yields, yet as the only crystalline solid-state product (via PXRD). Moreover, reactions involving gaseous CO_2 as a reagent were explored. Quantities of dry ice (~1 g) were placed into charged reaction vessels and allowed to sublime prior to heating, as described above. This was done for reactions with and without H_2pzdc. For the latter, no solid products were observed upon opening reaction vessels, and upon drying, only metal salts were recovered. For reactions involving CO_2 and H_2pzdc, no change in products was observed; that is, no pure oxalate phases or materials other than compound **1** were recovered. Lastly, reactions were also carried out under semi-inert conditions by bubbling Ar(g) through a charged reaction vessel (to remove dissolved oxygen) and quickly sealing. Although not rigorously oxygen-free, a significant decrease in the yield of **1** (to ~4.8%) was noted.

Structure Description. As shown in Figure 1, the crystal structure of **1** consists of monomers of Nd^{3+} metal centers linked via H_2pzdc and oxalate anions to form thick two-dimensional sheets. Each Nd^{3+} is nine-coordinate and is bound to three bidentate $pzdc^{2-}$ molecules, a bidentate oxalate ligand, and a water molecule. Two $pzdc^{2-}$ acid units are bound to the Nd(III) metal centers through N1 of the pyrazine ring and a carboxylate oxygen (O1) at distances of 2.874(3) and 2.389(2) Å, respectively, resulting in chains that propagate along [010]. The chains are further connected along [100] into two-dimensional sheets via coordination of Nd^{3+} to an additional H_2pzdc ligand through carboxylate oxygen atom O2 and its symmetry equivalent at a distance of 2.384(2) Å. Bidentate oxalate units complete the coordination sphere of Nd^{3+} and additionally connect the layers into thick two-dimensional sheets, as illustrated in Figure 1b.

Nuclear Magnetic Resonance Spectroscopy. Reaction conditions to produce **1** were scaled to fit NMR tubes for ex situ and in situ monitoring of the aqueous phase organic species. The following sections detail the ^{1}H and ^{13}C NMR studies.

Quenched Reactions in D_2O. From a stock solution of 80 mM $Nd(NO_3)_3{\cdot}6H_2O$ and 80 mM H_2pzdc in D_2O, six equivalent reactions were prepared. An aliquot of the solution was transferred to a 5 mm diameter NMR tube that was purged with argon gas and flame-sealed. The filling factor was 50%. ^{1}H and ^{13}C spectra of the initial solution were collected. The remaining samples were then placed into a furnace and heated statically at 120 °C. After 30 min, 1 h, 2 h, 3 h, 5 h, and 10 h, respectively, the reactions were cooled to 30 °C by immersing the tube in a water bath. ^{13}C spectra were collected at each time point. At the 5 and 10 h time points, ^{1}H- and ^{13}C-DEPT measurements were also performed. ^{13}C NMR measurements of the gas phase were also conducted by simply inverting the tube. ^{1}H and proton-decoupled ^{13}C NMR spectra were measured at 30 °C with a 400 MHz (JEOL ECA400) or a 600 MHz (JEOL ECA600) NMR.

Quenched Reactions in H_2O. A consequence of using D_2O in the studies reported above was that some protons of the decarboxylated and oxidized species were replaced by deuterium. As such, some peaks were not observable in the ^{1}H spectrum. Performing the reactions in water was also imperative for DEPT measurements, which indicate the type (if any) of proton(s) associated with a carbon atom. Reactions were thus prepared in distilled water to confirm our peak assignments. A stock solution of 80 mM $Nd(NO_3)_3{\cdot}6H_2O$ and 80 mM H_2pzdc in H_2O was prepared. An aliquot of the solution was transferred to a 5 mm diameter NMR tube that was then purged with argon gas and flame-sealed (the filling factor was 50%). ^{1}H and ^{13}C spectra of the initial solution were collected. The sample was then placed into an electric oven and heated statically at 120 °C for 5 h. After 5 h, the tube was immersed in a water bath and ^{13}C, ^{1}H, and DEPT measurements were performed.

High-Temperature ^{1}H NMR: In Situ Studies. ^{1}H and ^{13}C measurements were collected at Kyoto University on a 500 MHz system (JEOL JNM-ECA500) equipped with a wide-bore superconductor magnet (11.3 T) and a high-temperature NMR probe developed by Nakahara et al.[62] Neodymium nitrate hexahydrate (0.175 g, 0.39 mmol) and 2,3-pyrazinedicarboxylic acid (0.067 g, 0.40 mmol) were dissolved in 5 mL of D_2O. The resulting solution was transferred to a 5 mm diameter quartz tube to give a filling factor of 50% (total length 14 cm). The tube was then purged with argon gas and flame-sealed. ^{1}H and ^{13}C spectra of the unheated solution were collected at 30 °C (initial). The reaction was then heated to 120 °C, and once the temperature stabilized, a ^{1}H spectrum of the liquid phase was collected at 120 °C (time = 0). The reaction remained at 120 °C, and ^{1}H measurements of the solution were taken at 120 °C at 0.5 and 1, 2, 3, 4, 5, 6, 15, and 24 h time points. In one set of reactions, the solution was cooled to 30 °C after 15 h and ^{1}H and ^{13}C NMR spectra of the solution were collected.

RESULTS

The lanthanide elements are paramagnetic, and small changes in the chemical shifts of the ^{1}H NMR spectra are induced by these ions. Little effect is observed in the ^{13}C spectrum. The "lanthanide-induced shifts" are concentration-dependent. Prior to assigning the observed peaks, standards of various organic species over a range of metal/ligand ratios were run. Such standards allowed us to correlate the peaks in the observed spectrum with the hydrogen atoms of 2,3-pyrazinedicarboxylic

dx.doi.org/10.1021/ic3000944 | Inorg. Chem. 2012, 51, 3883−3890

acid and 2-pyrazinecarboxylic acid, in particular, as a function of concentration despite small changes in the chemical shift over time. The Spectral Database for Organic Compounds (SDBS), the Aldrich Library of ^{13}C and ^{1}H FT NMR spectra, and the predict ^{1}H and ^{13}C shifts function within ChemDraw Ultra 9.0 were used in addition to the standards for peak assignment. A list of species along with their chemical shifts are available in the Supporting Information. The mono- and dicarboxylate are depicted in Figure 2.

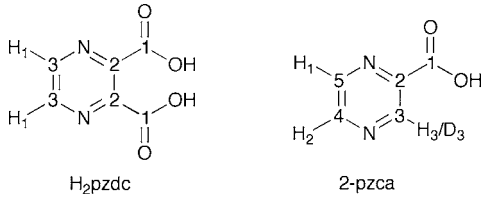

Figure 2. Illustration of the mono- (2-pzca) and dicarboxylate (H_2pzdc) ligands. The hydrogen and carbon atoms that are observed in the NMR spectra are labeled. H_2pzdc has two protons and three carbon nuclei in chemically unique environments, whereas 2-pzca has four unique protons and five distinct carbon nuclei.

The ^{1}H NMR spectra collected for the solution at 0, 5, and 10 h are shown in Figure 3. There are two peaks in the initial

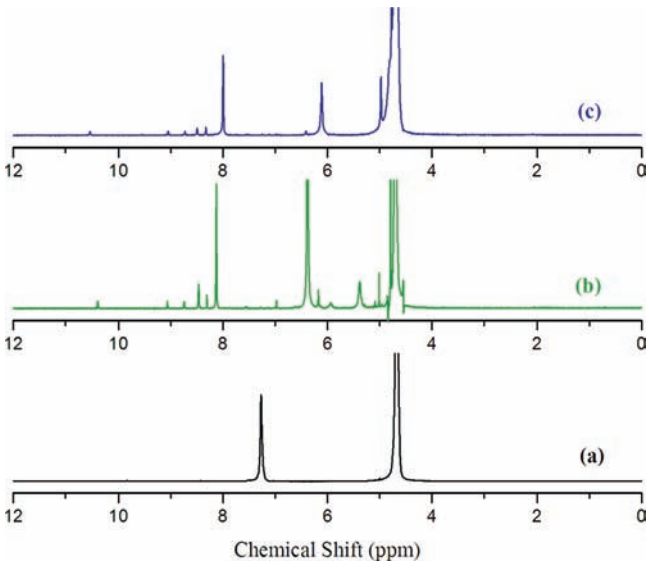

Figure 3. ^{1}H NMR spectra of a 80 mM H_2pzdc/80 mM $Nd(NO_3)_3$ solution in D_2O: (a) initial, (b) after 5 h at 120 °C, and (c) after 10 h at 120 °C. Spectra were collected at 30 °C and have been magnified to highlight the details of each spectrum.

spectrum (a). The peak at 4.68 ppm is attributed to H_2O, while the peak at 7.26 ppm can be assigned to the hydrogen atoms of the pyrazine ring of H_2pzdc (H1). Note that the −COOH hydrogen atoms are not observed, likely due to rapid H/D exchange. After 5 h (Figure 3b), peaks appear at 6.38 and 8.13 ppm that can be assigned to the hydrogen atoms of the pyrazine ring (H1 and H2) of the monocarboxylate, 2-pzca. We should expect to see three peaks attributed to the monocarboxylate, but, because the reaction is in D_2O, the site of decarboxylation is deuterated (D3) and no peak is observed. Peaks at 5.39 and 5.00 ppm are also observed and are likely attributed to glyoxylic and glycolic acids. Further, the peaks at 8−9 ppm are likely attributed to the free acid, and the broad peak at 5.9 is consistent with 2-hydroxymalonic acid. After 10 h, we see nearly complete disappearance of the peak attributed to the H_2pzdc unit. Peaks associated with the monocarboxylate are observed at 6.11 and 7.99 ppm. The peak at 4.97 is assigned to glycolic acid, and H_2O is observed at 4.67 ppm. These assignments are further supported by the ^{13}C NMR spectra. Note that no internal reference was used, but rather the sensitivity of the detector was kept constant during this experiment. Spectra were integrated, and normalized concentrations correspond to the ratio of the hydrolyzed/oxidized species against the initial H_2pzdc concentration. The mass balance is proton-based.

The ^{13}C NMR spectra collected at 0, 2, 5, and 10 h are shown in Figure 4. The H_2pzdc ligand has three unique carbon

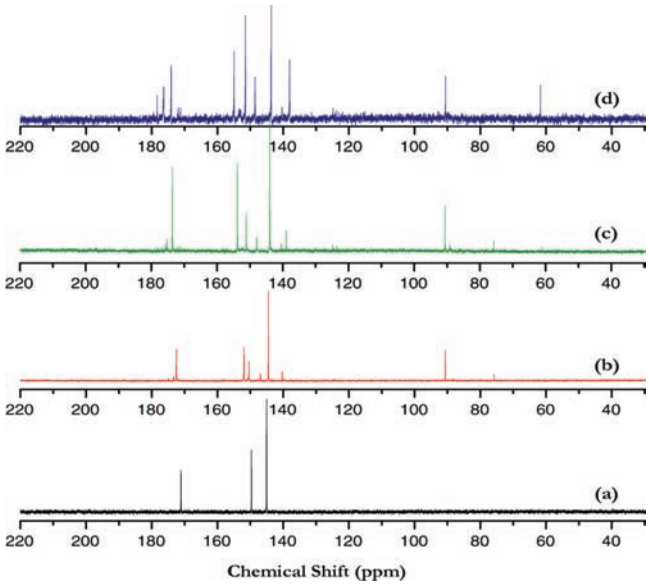

Figure 4. ^{13}C NMR spectra of 80 mM H_2pzdc + 80 mM $Nd(NO_3)_3$ solution in D_2O: (a) initial, (b) after 2 h at 120 °C, (c) after 5 h at 120 °C, and (d) after 10 h at 120 °C. All spectra were collected at 30 °C.

atoms, and as such, we see three peaks in the ^{13}C NMR. These peaks are observed at 171.0, 149.7, and 145.1 ppm in the initial spectrum (a). After 2 h (b), peaks attributed to the carbon atoms of the pyrazine ring (140−154 ppm) and −COOH (170−180 ppm) of both the mono- and dicarboxylate are present. Peaks at 75.7 and 90.6 ppm are attributed to 2-hydroxymalonic acid and glyoxal/glyoxylic acid, respectively. Small peaks at 61 and 124 ppm appear in the 5 h spectrum (c) and can be assigned to glycolic acid and dissolved CO_2(g). At 10 h, the tartronic acid species is absent and the peak attributed to glycolic acid at 61 ppm is more intense. It should be noted that the ^{13}C NMR spectrum of the gas phase after 1 h exhibited a peak at 124.5 ppm consistent with the formation of CO_2(g).

The ^{1}H NMR spectrum of reaction 2 was similar to that of reaction 1 (Figure 3); however, an additional peak at 10.5 ppm attributed to monocarboxylate is observed. The ^{13}C spectrum with the DEPT measurement at 5 h is shown in Figure 5. The spectrum is similar to that shown in Figure 4 with peaks observed at 62.17, 90.76, 124.8, 138.01, 140.96, 148.66, 151.61, 153.62, 154.93, 171.04, 171.79, 174.28, 176.15, 177.12, and 178.80 ppm. Peaks assignments are illustrated in Figure 5a. The DEPT measurement shown in Figure 5b provides additional

dx.doi.org/10.1021/ic3000944 | Inorg. Chem. 2012, 51, 3883−3890

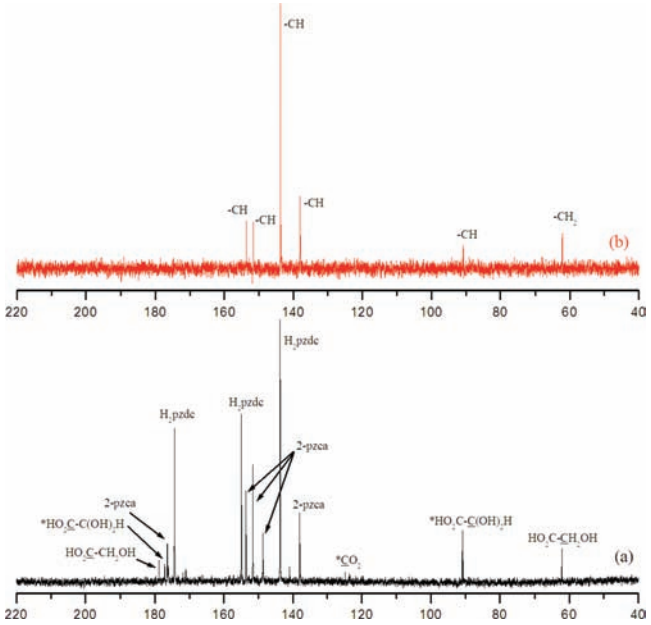

Figure 5. (a) ^{13}C NMR spectrum and (b) DEPT measurement of 80 mM H_2pzdc/80 mM $Nd(NO_3)_3$ solution in H_2O after 5 h at 120 °C. Both spectra were collected at 30 °C.

support for our assignments. The DEPT experiment determines the number of protons directly attached to the individual ^{13}C nucleus.[63] Only six ^{13}C nuclei have attached proton atoms (Figure 5). There are four CH peaks resulting from the pyrazine ring of 2-pzca and H_2pzdc. The peak at 90.76 is a CH peak consistent with glyoxylic acid, and the peak at 62.17 is a CH_2 peak attributed to glycolic acid.

For reaction 3, the ^{13}C spectrum collected for the solution after 15 h is shown in Figure 6. Peaks are observed at 61.91,

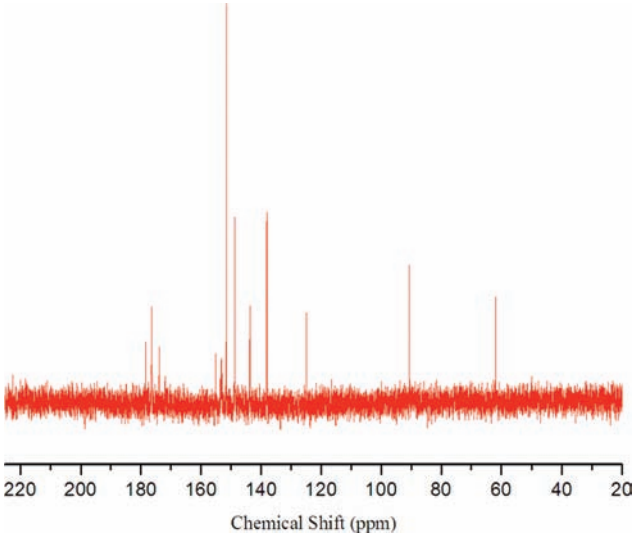

Figure 6. ^{13}CNMR spectrum for reaction of 80 mM $Nd(NO_3)_3{\cdot}6H_2O$ and 80 mM H_2pzdc in D_2O (pH 1) collected at 30 °C after 15 h at 120 °C.

90.64, 124.85, 138.11, 143.76, 148.75, 151.56, 153.22, 155.20, 174.00, 176.44, and 178.47 ppm. Perhaps the most notable peak is that at 124.85 ppm that is attributed to dissolved CO_2(g). The ^{1}H NMR spectrum is nearly identical to that shown in Figure 2.

DISCUSSION

The ^{13}C spectra of the quenched reactions (in both D_2O and H_2O) had peaks corresponding to the starting material, 2,3-pyrazinedicarboxylic acid (H_2pzdc), as well as a number of decomposition products. Observed decomposition products include 2-pyrazinecarboxylic acid (2-pzca), CO_2(g), 3-amino-2-hydroxy-3-oxopropanoic acid and/or 2-hydroxymalonic acid, glyoxal, glyoxylic acid, and glycolic acid. The ^{1}H NMR spectra and DEPT measurements supported these assignments. We therefore propose that under hydrothermal conditions and in the presence of Nd^{3+}, the oxalate anion is formed in situ via a ring-opening under the influence of metal−ligand coordination (Scheme 2). Prior to precipitation, the presence of metal

Scheme 2. A Proposed Route for the Formation of Oxalate Anions from 2,3-Pyrazinedicarboxylic Acid (H_2pzdc) via Pyrazine Ring-Opening[a]

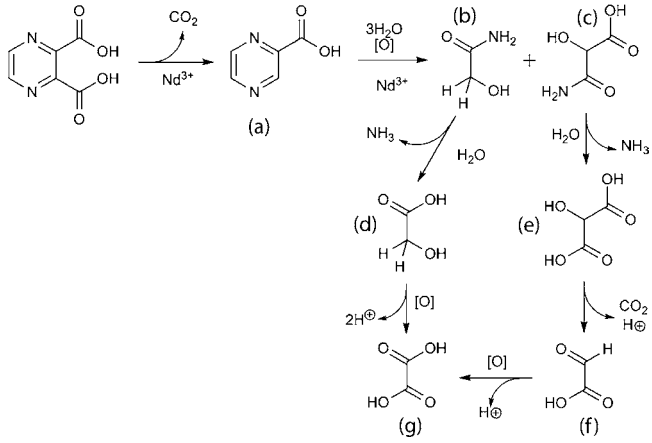

[a] H_2pzdc loses CO_2 to form 2-pyrazinecarboxylic acid (a), which subsequently undergoes a ring-opening to produce 2-hydroxyacetamide (b) and 3-amino-2-hydroxy-3-oxopropanoic acid (c). Hydrolysis of these species can give rise to glycolic acid (d), 2-hydroxymalonic acid (e), 2-oxoacetic acid (f), and ultimately oxalate anions (g). [O] is presumed to be dissolved oxygen in reaction mixtures.

cations, nitrogen lone pairs, and carboxylate chelation likely accelerate in situ ligand formation and control end product formation. Coloumbic interaction of the f-metal center with the H_2pzdc ligand facilitates decarboxylation to yield 2-pzca, observed in the ^{1}H and ^{13}C spectra, and CO_2(g), observed in the ^{13}C spectrum collected after 15 h. Further, cleavage of the C−N bond of the pyrazine ring is likely induced by fluctuations of the electron distribution between the metal ion and the ligand carboxylate to yield 2-hydroxyacetamide (b) and 3-amino-2-hydroxy-3-oxopropanoic acid; the hydrolysis products of these species (glycolic acid (d) and 2-hydroxymalonic acid (e)) are observed in the ^{1}H and ^{13}C NMR spectra.

Although quenched reactions (reactions 1 and 2) were useful in identifying product speciation, they are somewhat limiting. Such studies are subject to significant conditional changes. Temperature, for example, likely affects chemical speciation in the solution phase; those species present in solution under hydrothermal conditions (120 °C) are not necessarily soluble at room temperature (30 °C). In fact, it is common for products to precipitate out of solution upon cooling, as the solubility of

dx.doi.org/10.1021/ic3000944 | Inorg. Chem. 2012, 51, 3883−3890

these species decreases. Quenched reactions do not accurately render the solution as it exists under hydrothermal conditions as the organic speciation profiles at 30 and 120 °C are likely different. In situ observation of the reactions under nonambient conditions, however, provides direct information regarding chemical speciation that is arguably necessary to accurately rationalize and address mechanisms of ligand formation. The ^{1}H NMR spectra from the reaction of 80 mM $Nd(NO_3)_3$ and 80 mM H_2pzdc monitored at 120 °C as a function of time is shown in Figure 7. After 1 h, peaks corresponding to both

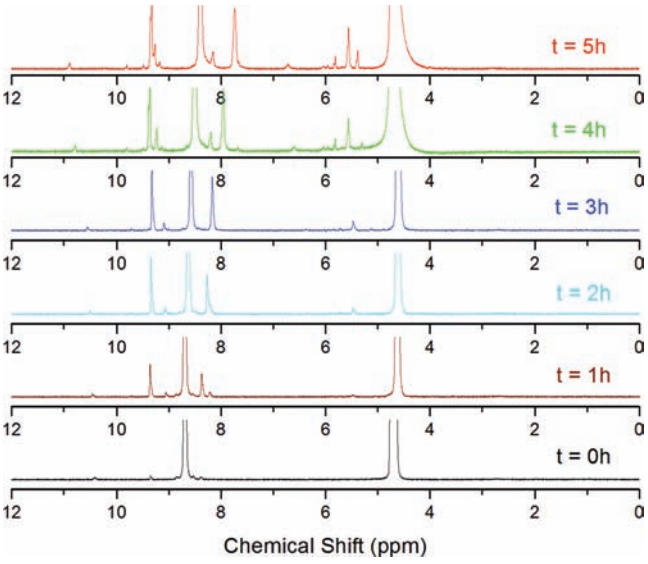

Figure 7. ^{1}H NMR spectra of a 80 mM H_2pzdc/80 mM $Nd(NO_3)_3$ solution after 0, 1, 2, 3, 4, and 5 h at 120 °C. The reaction was followed in situ, and spectra were collected at 120 °C. Note that the spectra have been magnified to highlight the details of each spectrum.

H_2pzdc and 2-pzca are observed. At 2 h, a peak at 5.5 ppm likely due to glyoxylic or glycolic acid begins to appear. After 5 h, H_2pzdc peaks are still present in the reaction solution and many other peaks are observed. The peaks at approximately 5.5 ppm are likely attributed to glyoxylic and glycolic acids. The peak at ~6.7 ppm may be attributed to 2-hydroxymalonic acid, yet this assignment is somewhat uncertain. However, we can uniquely assign the peaks corresponding to H_2pzdc and 2-pzca, and the time evolution of these species is shown in Figure 8. As the reactant (H_2pzdc) is depleted, the decarboxylated product (2-pzca) is evolved in the hydrothermal reaction of 80 mM $Nd(NO_3)$ and 80 mM H_2pzdc. The concentration of 2-pzca increases until ~300 min, after which it plateaus. The concentration of H_2pzdc decreases over time, and the species is nearly depleted after 15 h.

As mentioned previously, 2,3-pyrazinedicarboxylic acid (H_2pzdc) decarboxylates to form 2-pyrazinecarboxylic acid (2-pzca). It has also been proposed that this decarboxylation ($-CO_2$) of H_2pzdc and subsequent reductive coupling of CO_2 are responsible for the formation of oxalate ligands in situ.[49,51] The formation of both 2-pzca and CO_2(g) are observed, yet the latter does not appear to be relevant to in situ oxalate formation. Moreover, if oxalate anions were formed through the reductive coupling of CO_2, we could expect a time-dependent relationship between the changes in the H_2pzdc and 2-pzca concentrations. In other words, if the oxalate is generated directly from the "decarboxylated" CO_2 without further organic

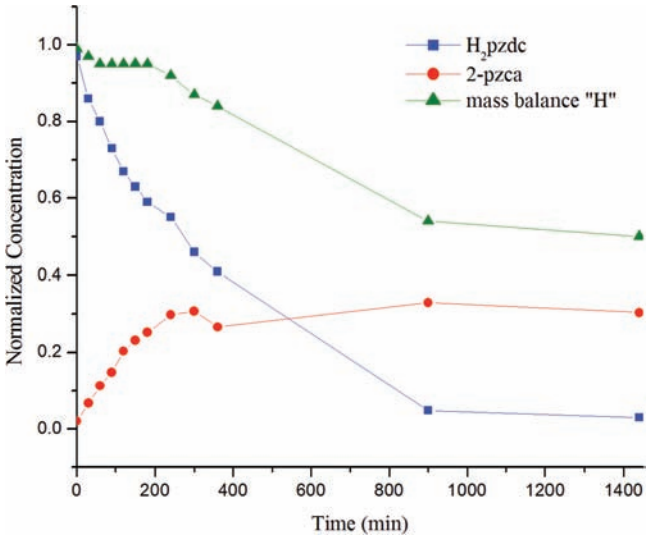

Figure 8. Time evolution of the H_2pzdc and 2-pzca yields for 80 mM $Nd(NO_3)_3 \cdot 6H_2O$ and 80 mM H_2pzdc in D_2O (pH 1) at 120 °C. The normalized concentration denotes the ratio of the 2-pzca concentration against the initial concentration of H_2pzdc. The mass balance is proton-based.

reactivity, a decrease in the concentration of H_2pzdc should be accompanied by a proportional increase in the concentration of 2-pzca. In looking at the time evolution of the H_2pzdc and 2-pzca yields shown in Figure 8, decreases in the concentration of H_2pzdc do not consistently correspond to increases in 2-pzca. Rather, after 300 min, the concentration of 2-pzca plateaus, suggestive of subsequent decomposition (i.e., ring-opening). Further, products indicative of the ring-opening, such as 2-hydroxymalonic acid, glyoxylic acid, and glycolic acid, are verified. Also of note is the fact that oxalate species were never definitively observed in solution ^{13}C NMR, likely due to immediate and quantitative reaction (and subsequent precipitation) with the Nd ions. This is consistent with the loss of mass balance after 300 min, which is likely attributed to precipitation of the reaction product and, therefore, loss of H_2O, H_2pzdc, and oxalate from the reaction solution.

Whereas the concentration relationship of H_2pzdc and 2-pzca over time admittedly cannot serve as a definitive indicator against reductive coupling of CO_2, it does suggest a more complex relationship between the organic acid and the oxalate observed in the final product. This evidence, coupled with the observation of reactive intermediates and the apparent absence of a reducing agent (as well as the lower yield in degassed experiments), strongly supports the proposed, oxidative reaction mechanism. Moreover, comments and speculation regarding the role(s) of metal ions in promoting these and related systems have been afoot for some time.[64,65] Interestingly, with the exception of 5-hydroxyisopthalic acid and those species known to undergo hydrolysis (tartaric acid and ascorbic acid), many of the organic species listed in Table S1 (Supporting Information) contain a C−N bond, and indeed Li et al.[36] speculate on a similar pathway. Whereas we hesitate to state definitively that each of these entries in Table S1 (Supporting Information) proceed by the mechanism proposed herein, it is entirely possible that a similar pathway of oxalate formation (i.e., a ring-opening) is present in these systems. The role of dissolved oxygen in hydro(solvo)thermal reaction

dx.doi.org/10.1021/ic3000944 | Inorg. Chem. 2012, 51, 3883−3890

mixtures likely requires more careful examination, but could conceivably serve as the oxidant for such mechanisms.[66,67]

CONCLUSION

Efforts to produce hybrid materials have traditionally focused on the assembly of inorganic subunits with intact linker molecules, many of which are chosen for their robust nature and ability to withstand hydrothermal conditions. In situ ligand formation, a phenomenon that is being reported with increasing frequency, is a departure from this approach in that reactivity within the linker molecules results in (often) unanticipated reaction products. Consequently, mechanistic information has typically been implied and obtained through ex situ analyses. This study, however, marks an effort to probe oxalate formation pathways directly via in situ NMR spectroscopy. We investigated oxalate ligand formation under hydrothermal conditions, not with the aim of producing new materials, but for gaining a better understanding of formation mechanisms. Reactions of $Nd(NO_3)_3$ and H_2pzdc known to yield a Nd-oxalate were examined using ^1H and ^{13}C NMR. We have proposed that the decomposition of H_2pzdc proceeds through an oxidative pyrazine ring-opening to yield intermediates, such as 2-pyrazinecarboxylic acid (2-pzca), 2-hydroxyacetamide, 3-amino-2-hydroxy-3-oxopropanoic acid, 2-hydroxymalonic acid, glyoxylic acid, and glycolic acid. The oxalate ligands are then observed in the crystalline reaction product $Nd_2(C_6H_2N_2O_4)_2(C_2O_4)(H_2O)_2$. In contrast to many previous reports (including our own), we note that the CO_2 liberated by decarboxylation does *not* participate in oxalate formation. Using this approach, we hope to understand metal−organic interactions/redox/speciation more thoroughly and, in turn, capitalize on organic reactivity in parallel with more traditional assembly routes.

ASSOCIATED CONTENT

Supporting Information

Table of oxalate ligand formation under hydro(solvo)thermal conditions and ^1H and ^{13}C NMR chemical shifts, This material is available free of charge via the Internet at http://pubs.acs.org.

AUTHOR INFORMATION

Corresponding Author

*E-mail: cahill@gwu.edu (C.L.C.).

Notes

The authors declare no competing financial interest.

ACKNOWLEDGMENTS

Researchers at GW were supported by the National Science Foundation (DMR- 0348982) and the U.S. Department of Energy (DOE) under Grant DE-FG02-05ER15736. K.E.K. is particularly grateful for the support of the NSF-East Asia-Pacific Summer Institute (EAPSI) program that allowed her to travel to Kyoto to collaborate with Professor Nakahara's group. Researchers at Kyoto are supported by The Japan Society for The Promotion of Science (JSPS) for the counterpart of EAPSI.

REFERENCES

(1) Ockwig, N. W.; Delgado-Friedrichs, O.; O'Keeffe, M.; Yaghi Omar, M. *Acc. Chem. Res.* **2005**, *38*, 176−82.
(2) Allen, F. H. *Acta Crystallogr., Sect. B: Struct. Sci.* **2002**, *B58*, 380−388 . Cambridge Structure Database, Version 5.24, November 2004.
(3) Férey, G. *Dalton Trans.* **2009**, 4400−4415.
(4) Férey, G. *Chem. Soc. Rev.* **2008**, *37*, 191−214.
(5) Horcajada, P.; Serre, C.; Vallet-Regí, M.; Sebban, M.; Taulelle, F.; Férey, G. *Angew. Chem., Int. Ed.* **2006**, *45*, 5974−5978.
(6) Kitagawa, S.; Matsuda, R. *Coord. Chem. Rev.* **2007**, *251*, 2490−2509.
(7) Kitagawa, S.; Noro, S.-i.; Nakamura, T. *Chem. Commun.* **2006**, 701−707.
(8) Kitagawa, S.; Uemura, K. *Chem. Soc. Rev.* **2005**, *34*, 109−119.
(9) Batten, S. R.; Robson, R. *Angew. Chem., Int. Ed.* **1998**, *37*, 1461−1494.
(10) Wang, Z.; Cohen, S. M. *J. Am. Chem. Soc.* **2007**, *129*, 12368−12369.
(11) Eddaoudi, M.; Kim, J.; Rosi, N.; Vodak, D.; Wachter, J.; O'Keeffe, M.; Yaghi, O. M. *Science* **2002**, *295*, 469−72.
(12) Rosi, N. L.; Eckert, J.; Eddaoudi, M.; Vodak, D. T.; Kim, J.; O'Keeffe, M.; Yaghi, O. M. *Science* **2003**, *300*, 1127−1130.
(13) Cahill, C. L.; de Lill, D. T.; Frisch, M. *CrystEngComm* **2007**, *9*, 15−26.
(14) Allendorf, M. D.; Bauer, C. A.; Bhakta, R. K.; Houk, R. J. T. *Chem. Soc. Rev.* **2009**, *38*, 1330−1352.
(15) Hill, R. J.; Long, D.-L.; Hubberstey, P.; Schroder, M.; Champness, N. R. *J. Solid State Chem.* **2005**, *178*, 2414−2419.
(16) James, S. L. *Chem. Soc. Rev.* **2003**, *32*, 276−288.
(17) Janiak, C. *Dalton Trans.* **2003**, 2781−2804.
(18) Chen, X.-M.; Tong, M.-L. *Acc. Chem. Res.* **2007**, *40*, 162−170.
(19) Zhang, X.-M. *Coord. Chem. Rev.* **2005**, *249*, 1201−1219.
(20) Zheng, N.; Bu, X.; Feng, P. *J. Am. Chem. Soc.* **2002**, *124*, 9688−9689.
(21) Liu, C.-M.; Gao, S.; Kou, H.-Z. *Chem. Commun.* **2001**, 1670−1671.
(22) Tao, J.; Zhang, Y.; Tong, M.-L.; Chen, X.-M.; Tan, Y.; Lin, C. L.; Huang, X.; Li, J. *Chem. Commun.* **2002**, 1342−1343.
(23) Zhang, J.-P.; Lin, Y.-Y.; Huang, X.-C.; Chen, X.-M. *J. Am. Chem. Soc.* **2005**, *127*, 5495−5506.
(24) Cheng, L.; Zhang, W.-X.; Ye, B.-H.; Lin, J.-B.; Chen, X.-M. *Inorg. Chem.* **2007**, *46*, 1135−1143.
(25) Xiong, R.-G.; Xue, X.; Zhao, H.; You, X.-Z.; Abrahams, B. F.; Xue, Z. *Angew. Chem., Int. Ed.* **2002**, *41*, 3800−3803.
(26) Knope, K. E.; Cahill, C. L. *CrystEngComm* **2011**, *13*, 153−157.
(27) Zhu, H.-B.; Li, L.; Xu, G.; Gou, S.-H. *Eur. J. Inorg. Chem.* **2010**, *2010*, 1143−1148.
(28) Zhang, Y.-N.; Wang, Y.-Y.; Hou, L.; Liu, P.; Liu, J.-Q.; Shi, Q.-Z. *CrystEngComm* **2010**, *12*, 3840−3851.
(29) Han, L.; Bu, X.; Zhang, Q.; Feng, P. *Inorg. Chem.* **2006**, *45*, 5736−5738.
(30) Rowland, C. E.; Belai, N.; Knope, K. E.; Cahill, C. L. *Cryst. Growth Des.* **2010**, *10*, 1390−1398.
(31) Hix, G. B.; Kariuki, B. M.; Kitchin, S.; Tremayne, M. *Inorg. Chem.* **2001**, *40*, 1477−1481.
(32) Evans, O. R.; Lin, W. *Acc. Chem. Res.* **2002**, *35*, 511−522.
(33) Knope, K. E.; Cahill, C. L. *Eur. J. Inorg. Chem.* **2010**, *2010*, 1177−1185.
(34) Hou, J.-J.; Zhang, X.-M. *Cryst. Growth Des.* **2006**, *6*, 1445−1452.
(35) Zhang, Z.-J.; Zhang, S.-Y.; Li, Y.; Niu, Z.; Shi, W.; Cheng, P. *CrystEngComm* **2010**, *12*, 1809−1815.
(36) Li, X.; Cao, R.; Sun, D.; Shi, Q.; Bi, W.; Hong, M. *Inorg. Chem. Commun.* **2003**, *6*, 815−818.
(37) Nadeem, M. A.; Bhadbhade, M.; Bircher, R.; Stride, J. A. *Cryst. Growth Des.* **2010**, *10*, 4060−4067.
(38) Sun, Y.-Q.; Zhang, J.; Yang, G.-Y. *Chem. Commun.* **2006**, 1947−1949.
(39) Jiang, Y.-S.; Yu, Z.-T.; Liao, Z.-L.; Li, G.-H.; Chen, J.-S. *Polyhedron* **2006**, *25*, 1359−1366.
(40) Han, Z.-B.; Cheng, X.-N.; Li, X.-F.; Chen, X.-M. *Z. Anorg. Allg. Chem.* **2005**, *631*, 937−942.
(41) Yigit, M. V.; Wang, Y.; Moulton, B.; MacDonald, J. C. *Cryst. Growth Des.* **2006**, *6*, 829−832.

(42) Yu, X.-Y.; Ye, L.; Zhang, X.; Cui, X.-B.; Zhang, J.-P.; Xu, J.-Q.; Hou, Q.; Wang, T.-G. *Dalton Trans.* **2010**, *39*, 10617−10625.
(43) Hu, X.-X.; Xu, J.-Q.; Cheng, P.; Chen, X.-Y.; Cui, X.-B.; Song, J.-F.; Yang, G.-D.; Wang, T.-G. *Inorg. Chem.* **2004**, *43*, 2261−2266.
(44) Blake, A. J.; Champness, N. R.; Chung, S. S. M.; Li, W.-S.; Schroder, M. *Chem. Commun.* **1997**, 1675−1676.
(45) Li, X.; Pecoraro, V. L. *Inorg. Chem.* **1989**, *28*, 3403−3410.
(46) Belsky, A. J.; Maiella, P. G.; Brill, T. B. *J. Phys. Chem. A* **1999**, *103*, 4253−4260.
(47) Frisch, M.; Cahill, C. L. *J. Solid State Chem.* **2007**, *180*, 2597−2602.
(48) Frisch, M.; Cahill, C. L. *Dalton Trans.* **2006**, 4679−4690.
(49) Ziegelgruber, K. L.; Knope, K. E.; Frisch, M.; Cahill, C. L. *J. Solid State Chem.* **2008**, *181*, 373−381.
(50) Knope, K. E.; Cahill, C. L. *Inorg. Chem.* **2007**, *46*, 6607−6612.
(51) Soares-Santos, P. C. R.; Cunha-Silva, L.; Paz, F. A. A.; Ferreira, R. A. S.; Rocha, J.; Carlos, L. D.; Nogueira, H. I. S. *Inorg. Chem.* **2010**, *49*, 3428−3440.
(52) Hausdorf, S.; Baitalow, F.; Seidel, J.; Mertens, F. O. R. L. *J. Phys. Chem. A* **2007**, *111*, 4259−4266.
(53) Bakhmutov, V. I. *Chem. Rev.* **2011**, *111*, 530−562.
(54) Pienack, N.; Bensch, W. *Angew. Chem., Int. Ed.* **2011**, *50*, 2014−2034.
(55) Cheetham, A. K.; Mellot, C. F. *Chem. Mater.* **1997**, *9*, 2269−2279.
(56) Li, J.; Brill, T. B. *J. Phys. Chem. A* **2003**, *107*, 5987−5992.
(57) Brill, T. B. *J. Phys. Chem. A* **2000**, *104*, 4343−4351.
(58) Yasaka, Y.; Yoshida, K.; Wakai, C.; Matubayasi, N.; Nakahara, M. *J. Phys. Chem. A* **2006**, *110*, 11082−11090.
(59) Nagai, Y.; Morooka, S.; Matubayasi, N.; Nakahara, M. *J. Phys. Chem. A* **2004**, *108*, 11635−11643.
(60) Wakai, C.; Yoshida, K.; Tsujino, Y.; Matubayasi, N.; Nakahara, M. *Chem. Lett.* **2004**, *33*, 572−573.
(61) Morooka, S.; Wakai, C.; Matubayasi, N.; Nakahara, M. *J. Phys. Chem. A* **2005**, *109*, 6610−6619.
(62) Yoshida, K.; Matubayasi, N.; Nakahara, M.; Ikeda, T.; Anai, T. *JEOL News* **2007**, *42E*.
(63) Silverstein, R. M.; Bassler, G. C.; Moril, T. C. *Spectrometric Identification of Organic Compounds*, 5th ed.; John Wiley & Sons, Inc.: New York, 1991; pp 16−20.
(64) Lerner, E. I.; Lippard, S. J. *Inorg. Chem.* **1977**, *16*, 1546−1551.
(65) Bu, X.-H.; Liu, H.; Du, M.; Zhang, L.; Guo, Y.-M.; Shionoya, M.; Ribas, J. *Inorg. Chem.* **2002**, *41*, 1855−1861.
(66) Rowland, C. E.; Cantos, P. M.; Toby, B. H.; Frisch, M.; Deschamps, J. R.; Cahill, C. L. *Cryst. Growth Des.* **2011**, *11*, 1370−1374.
(67) Carril, M.; SanMartin, R.; Dominguez, E.; Tellitu, I. *Green Chem.* **2007**, *9*, 315−317.